

Comparison of ultrasound colored image views produced by application of statistical analysis of radio-frequency signals and histological findings in patients with chronic hepatitis C

Sanae Nakajima · Kazutoshi Shibuya ·
Naohisa Kamiyama · Yasukiyo Sumino

Received: 14 May 2009 / Accepted: 7 August 2009 / Published online: 11 December 2009
© The Japan Society of Ultrasonics in Medicine 2009

Abstract

Purpose To assess the tissue characteristics of chronic liver disease, we statistically analyzed the speckle signal from liver parenchyma.

Subjects and methods Analysis was performed for 65 patients with biopsy-proven chronic hepatitis C; individuals with fatty liver, heavy drinkers, and those with a thick abdominal wall were excluded. The probability density function of radio-frequency signal amplitude was statistically analyzed using a new analytical method. We focused on strong signals which deviated remarkably from the Rayleigh distribution. By applying the analytical results, lesions that caused the strong signals were displayed as red scatter overlaid on B-mode images (we called the red scatter “US-Red” in this study). US-Red% occupancy on

the color image was statistically compared with pathological findings.

Results US-Red suggests the existence of an acoustic reflectional plane mainly formed of fibrous bridge and septa. US-Red% increased significantly with progression of liver fibrosis stage. US-Red% varied widely in cirrhosis, and US-Red% in the large nodule group was significantly higher than that in the small nodule group.

Conclusion The results suggest that US-Red% is useful for evaluating liver fibrosis stage (F1–3) and the size of nodules in cirrhosis. In addition, visually detecting the acoustic reflectional plane, which increases with progression of disease, as color images will be clinically beneficial.

Keywords Tissue characterization · Speckle · Acoustic reflectional plane · Probability density function · Rayleigh distribution

This paper was partially presented at the 19th Kanto Koshinetsu Regional Meeting of the Japan Society of Ultrasonics in Medicine, the 81st General Conference of the Japan Society of Ultrasonics in Medicine, and the 20th Kanto Koshinetsu Regional Meeting of the Japan Society of Ultrasonics in Medicine.

S. Nakajima (✉) · Y. Sumino
Division of Gastroenterology and Hepatology,
Department of Internal Medicine,
Toho University Omori Medical Center,
6-11-1 Omorinishi, Ota, Tokyo 143-8541, Japan
e-mail: sunny200x@hotmail.com

K. Shibuya
Department of Pathology,
Toho University Omori Medical Center,
6-11-1 Omorinishi, Ota, Tokyo 143-8541, Japan

N. Kamiyama
Ultrasound Systems Division, Toshiba Medical Systems Corp,
1385 Shimo-ishigami, Otawara, Tochigi 324-8550, Japan

Introduction

As a hepatic lesion progresses in cases of chronic viral liver disease, remodeling of the hepatic lobular architecture advances through fiber prolongation and nodule formation, resulting in sclerosis and atrophy of the entire liver. These changes are clinically reflected by ascites and the formation of collaterals, due to portal hypertension, thereby increasing the incidence of liver cancer. In view of this, paying close attention to sequential changes in hepatic lesions is critical to management of patients with chronic liver disease. Thus, attempts have been made to compare ultrasound findings and pathological findings [1–5] and to analyze hematological and biochemical data, etc. We, also, have made various attempts [6–10]. Despite these attempts,

liver biopsy is still required for a definitive diagnosis of liver disease. Because liver biopsy is invasive, a less invasive diagnostic method is needed in routine clinical practice.

In recent years, tissue characterization of the liver has been used as a simple, objective alternative to liver biopsy; this involves statistical analysis of the speckle signal from the liver parenchyma [11–17]. The results from these studies have revealed there is a correlation between histological changes and acoustic characteristics, although acoustic characteristics have not yet been applied in clinical practice. This study was thus undertaken to establish an ultrasound method for evaluating liver tissue changes from a more clinical viewpoint. To this end, the speckle signal was analyzed by the method of Yamaguchi et al. [11–14], and the findings thus obtained were compared with histopathological findings.

Subjects and methods

Subjects

The subjects in this study were 65 of 70 patients with chronic HCV-related liver disease who underwent abdominal ultrasonography and percutaneous liver biopsy at the Toho University Omori Medical Center during the 9-month period from November 2007 to July 2008. Liver fibrosis was staged as F1 in 15 cases, F2 in 16 cases, F3 in 12 cases, and F4 in 22 cases according to the New Inuyama Classification [18]. Histopathological diagnosis was made by two pathologists certified by the Japanese Society of Pathology, and those for whom diagnoses by the two pathologists were consistent with each other were enrolled in this study. Of the 70 patients, one with histologically proven fatty liver was excluded from the study because intense reflection and scattering by fat droplets may have affected the analytical results. One heavy drinker was also excluded from the study because of the possible effect of alcoholic liver fibrosis on the study. Three other patients with abdominal wall thickness >2 cm were also excluded from the study because it would be impossible to visualize the area of liver parenchyma required for the analysis within the image frame when the image is enlarged for detailed analysis.

Method of ultrasound imaging (raw data)

The ultrasonograph used was an SSA-790A (AplioXG, Toshiba Medical Systems, Otawara, Japan) combined with a PVT-674BT transducer (convex type, central frequency 6.0 MHz). Images were recorded in the form of signals (reflective waves from the tissue perceived by the

transducer) before being processed in various ways by the ultrasonograph. That is, radio-frequency (RF) signals were recorded and analyzed. In this way, it was possible to analyze the acoustic characteristics of the liver tissue. As a rule, the recording was conducted during fasting early in the morning. The images for analysis were taken from the liver parenchyma (from the right intercostal region to the right lobe S5 region) while avoiding vessels as far as possible. For detailed analysis, the images were enlarged to make the depth range at 4 cm, with the focus set at 3 cm. After completion of the test, the visual information (RF signals) was fed into a personal computer for analysis with special software developed using the C++ language.

Analytical method

The principle used for analysis in this study was based on the acoustical structure qualification (ASQ) method developed by Yamaguchi et al. [11–14] for statistical analysis of the probability density function (PDF) of RF signal amplitude. The principle is briefly presented below.

A region of interest (ROI) is set within the liver parenchyma on the image taken, and the PDF is calculated for the RF signal amplitude within the ROI. Thus the calculated PDF is known to be approximated by the Rayleigh distribution if the ROI contains only speckle signals and is free of any tissue structure higher than the spatial resolution level [19]. If fibers increase as a result of progression of liver disease to chronic hepatitis or liver cirrhosis, PDF is considered to deviate from the Rayleigh distribution. With the conventional method of PDF analysis, however, only one ROI was set within the image. As a result, if the ROI contained large structures (e.g., blood vessels) even when containing no fibers, or if the echo signal intensity within the ROI was non-homogeneous because of the effect of attenuation, the PDF form tended to deviate from the Rayleigh distribution. To resolve these problems and to improve the precision of analysis, the ASQ method was specifically designed as follows. If the examiner sets a large ROI within the liver, hundreds of small ROIs are automatically set within the large ROI (Fig. 1). Then, PDF calculation and analysis of deviation from the Rayleigh distribution are carried out on each of these multiple small ROIs. The degree of deviation is calculated as the ratio of the actual RF signal variance to the mean variance for the multiple small ROIs. The degree of deviation is equal to 100% if PDF is consistent with the Rayleigh distribution. Such local analysis with small ROIs can reduce the variance in analytical results arising from attenuation or the presence of unnecessary structures (a problem with conventional methods of analysis) [14]. It is not affected by attenuation due to a thick abdominal wall (containing subcutaneous fat), because this method does

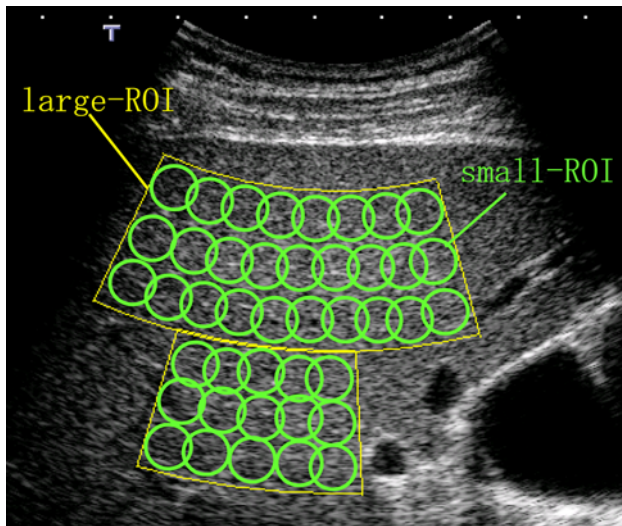


Fig. 1 Schematic diagram of ROIs for statistical analysis of RF signal with the ASQ method: several hundred small ROIs are set automatically in a large ROI

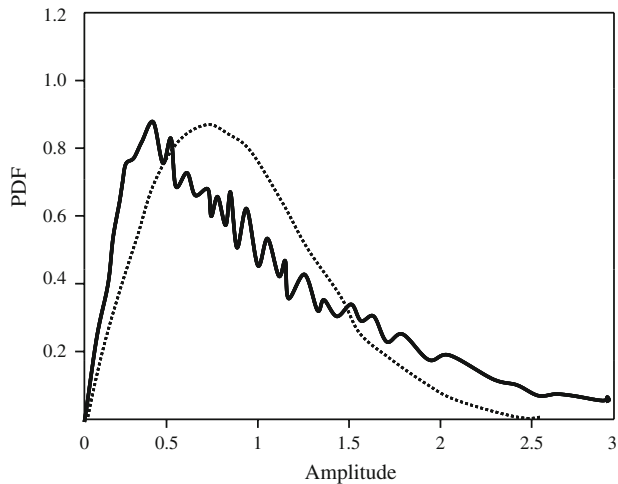


Fig. 2 Examples of PDF of amplitude: the signal amplitude is shown on the horizontal axis and the probability (frequency) on the vertical axis. The broken line shows the Rayleigh distribution. The echo signal PDF from normal liver substance almost corresponds to the Rayleigh distribution. In cirrhosis (solid line), signals of high amplitude are more abundant than for normal liver

not involve comparison of the signal amplitude itself but analyzes the ratio of variance. The manipulations and steps needed for this analysis are quite simple, and the results are not dependent on the examiner’s skill level.

A representative PDF for liver cirrhosis is presented in Fig. 2. The horizontal axis indicates the signal amplitude and the vertical axis refers to the probability (frequency). Compared with the theoretical Rayleigh distribution (shown as the broken line), the PDF for the case of liver cirrhosis, shown as the solid line, showed a shift of the peak to the lower level and tended to contain many

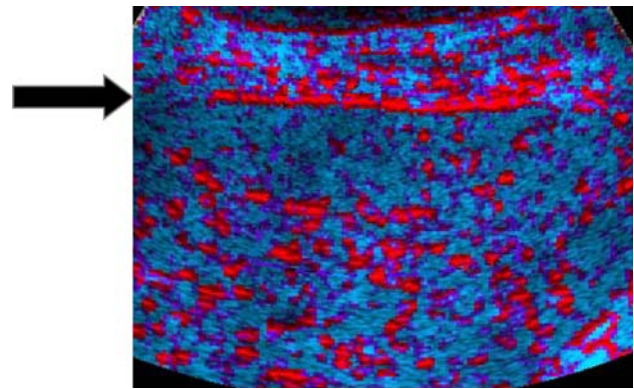


Fig. 3 Color image of liver parenchyma. The arrow indicates the liver surface. The red scatter (US-Red), which signifies the small ROIs that deviated from the Rayleigh distribution by 200% or more according to the ASQ method, are overlaid on the B-mode image

high-level signal amplitudes almost absent from the theoretical Rayleigh distribution.

Following this finding, we paid close attention to small ROIs showing marked deviation from the normal case (the theoretical Rayleigh distribution). To analyze the distribution of these small ROIs within the liver, we used computer program specifically developed for this purpose (making use of the above-mentioned principle of ASQ). With this program, the small ROIs showing a degree of deviation higher than the cut-off level were represented in red overlaid on B-mode images (Fig. 3). In this study, the diameter of each small ROI was set at about 1 mm, approximately equal to the liver nodule level, and the cut-off level was set at 200%. The red scatter thus obtained on B-mode images was called “US-Red”.

To objectively compare the share of US-Red, the percentage of the analyzed region of a B-mode image occupied by the US-Red was calculated (US-Red%). The analyzed region of a B-mode image was set in the vicinity of the focused area with dimensions of 1.75×1.75 cm.

Comparison of US-Red% and histopathological findings

1. Comparison with fibrosis stage

The relationship between US-Red% and the liver fibrosis stage was examined.

2. Comparison with percent liver fibrosis

The relationships between percent liver fibrosis and both liver fibrosis stage and US-Red% were analyzed. Percent liver fibrosis was calculated in the following way.

The liver biopsy specimen was photographed under a light microscope (magnification 40×) after Elastica van Gieson (EVG) staining, and the image was recorded in JPEG format. This image was converted with Photoshop

into a gray-scale image, followed by binarization at a cut-off level of 128 to represent only fibrous tissue. Then, using ImageJ, the percentage of fibrous tissue was calculated by comparing the total fibrous tissue area with the entire specimen area. This percentage was used as percent liver fibrosis in this study.

3. Classification of nodule size and fibrous septum thickness in cases of F4s

On the basis of the findings from EVG-stained liver biopsy specimens, nodule size and fibrous septum thickness for 22 F4 cases were classified and their correlation with US-Red% was analyzed.

Nodule size was classified into three categories: small group (cases predominantly having small nodules <3 mm in diameter), large group (cases predominantly having large nodules over 3 mm in diameter), and mixed group (cases having both large and small nodules). Fibrous septum was divided into three categories: thick group (cases predominantly having thick septum over 1 mm in thickness), thin group (cases predominantly having thin septum), and mixed group (cases having both thick and thin septum). US-Red% was analyzed in relation to nodule size and fibrous septum thickness.

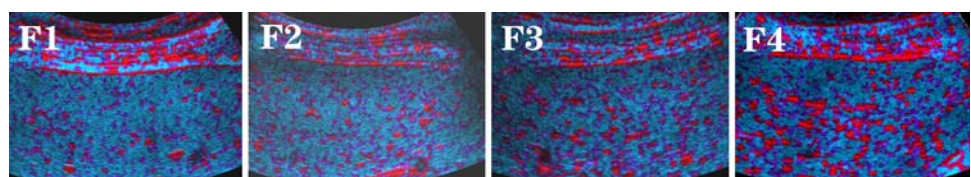
Statistical analysis

Spearman's correlation coefficient was used for analysis of the correlation between US-Red% and liver fibrosis stage and between liver fibrosis stage and percent liver fibrosis. Pearson's correlation coefficient was used for analysis of the correlation between US-Red% and percent liver fibrosis. Tukey's multiple comparison was used for testing the statistical significance of inter-group differences in US-Red% and nodule size and fibrous septum thickness in cases of F4. In all tests, $P < 0.05$ was regarded as statistically significant. Data are expressed as median value (minimum value–maximum value are reported in parentheses).

Informed consent and ethical considerations

Each patient was informed about the study design and enrolled in the study after his/her consent to the study and utilization of data for research was obtained. The protocol for this study was approved in advance by the Ethics Committee of our hospital.

Fig. 4 Color image: US-Red increases as the liver fibrosis stage (F1–F4) progresses



Results

US-Red% analyzed in relation to liver fibrosis stage

When US-Red% was analyzed in relation to liver fibrosis stage, median US-Red% was 5.2 (2.9–6.1) % for F1, 7.1 (4.1–9.3) % for F2, 8.7 (5.1–12.5) % for F3, and 8.9 (3.6–15.7) % for F4. Thus, US-Red on B-mode image tended to be more abundant with progression of liver fibrosis stage (Fig. 4). US-Red% increased significantly as the liver fibrosis stage progressed ($P = 0.70$, $P < 0.001$; Fig. 5). However, the US-Red% results varied widely in cases of F4. When cases of F4 were excluded from the analysis and only cases of F1 through F3 were analyzed, a stronger positive correlation was noted between US-Red% and liver fibrosis stage ($P = 0.76$, $P < 0.0001$).

US-Red% analyzed in relation to percent liver fibrosis

When percent liver fibrosis was analyzed in relation to liver fibrosis stage, Percent liver fibrosis was 2.1 (0.8–6.7) % for F1, 3.7 (2–7.7) % for F2, 8.8 (5.3–12.2) % for F3, and 13.8 (2.8–18) % for F4. Thus, percent liver fibrosis increased significantly as the liver fibrosis stage progressed ($P = 0.85$, $P < 0.001$; Fig. 6a). US-Red% tended to increase with increasing percent liver fibrosis, but the correlation was not statistically significant ($P = 0.18$; Fig. 6b).

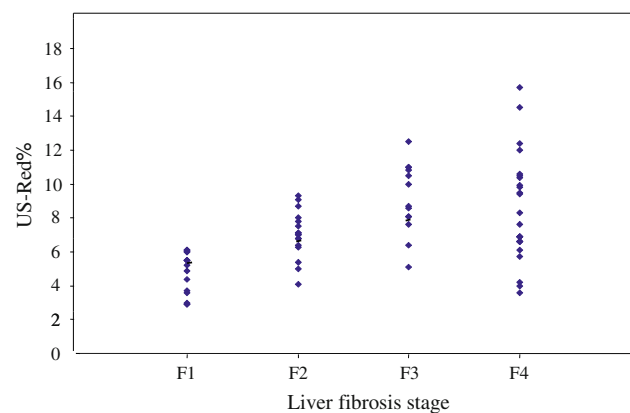


Fig. 5 Relationship between US-Red% and liver fibrosis stage (F1–F4) in patients with hepatitis C. There was a significant positive correlation ($\rho = 0.70$, $P < 0.001$, Spearman's correlation coefficient by rank)

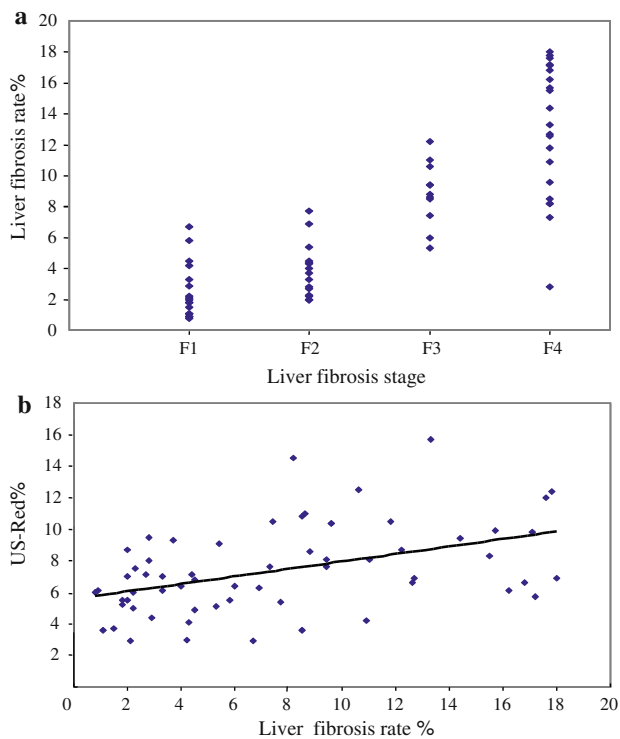


Fig. 6 **a** Relationship between percent liver fibrosis and liver fibrosis stage (F1–F4). There was a significant positive correlation ($\rho = 0.85$, $P < 0.001$, Spearman’s correlation coefficient by rank). **b** Relationship between US-Red% and percent liver fibrosis. There was no significant correlation ($P = 0.18$, Pearson’s correlation coefficient)

US-Red% analyzed in relation to nodule size and fibrous septum thickness in cases of F4

Because the results of US-Red% varied widely in cases of F4 ($n = 22$), we histologically divided these cases according to nodule size and fibrous septum thickness.

Nodule size was small in six cases, mixed in nine cases, and large in seven cases. When US-Red% was analyzed in relation to nodule size, US-Red% was 6.6 (3.6–8.3) % in the small group, 6.9 (4.2–14.5) % in the mixed group, and 9.9 (9.4–15.7) % in the large group. Thus, US-Red% differed significantly depending on nodule size ($P = 0.016$). That is, there were significant differences in US-Red% between the small group and the large group ($P < 0.05$; Fig. 7a), although there were no significant differences in US-Red% between the small group and the mixed group or between the mixed group and the large group.

Fibrous septum thickness was thin in ten cases, mixed in seven cases, and thick in five cases. When US-Red% was analyzed in relation to fibrous septum thickness, US-Red% was 6.8 (3.6–10.6) % in the thin group, 9.9 (6.1–15.7) % in the mixed group, and 9.8 (6.9–14.5) % in the thick group. US-Red% tended to increase as the septum became thicker, but there were no significant differences in US-Red%

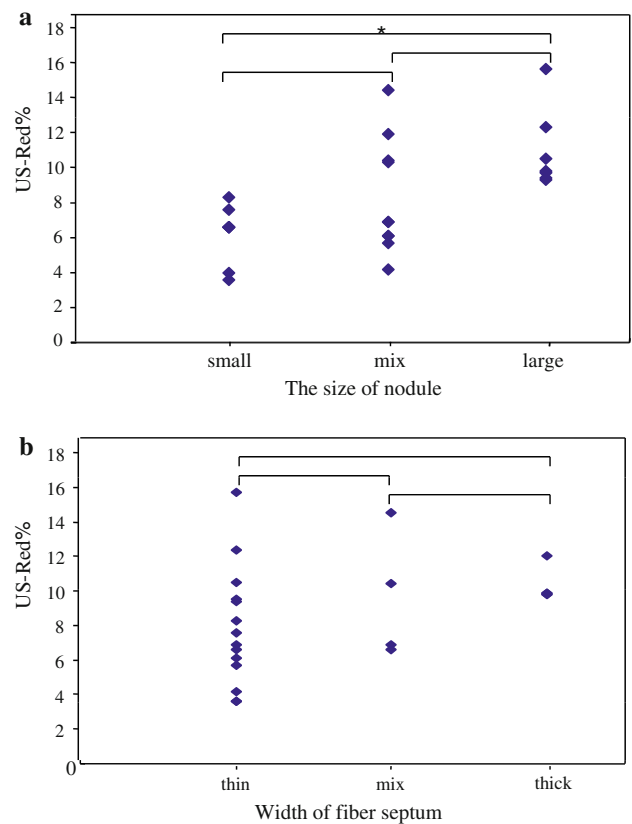


Fig. 7 **a** Comparison of US-Red% for three groups by size of nodule in cirrhosis. There was a significant difference among the three groups, and between the small group and the large group ($*P < 0.05$, Turkey test). **b** Comparison of US-Red% for three groups by width of fiber septum in cirrhosis. There was no significant difference among the three groups

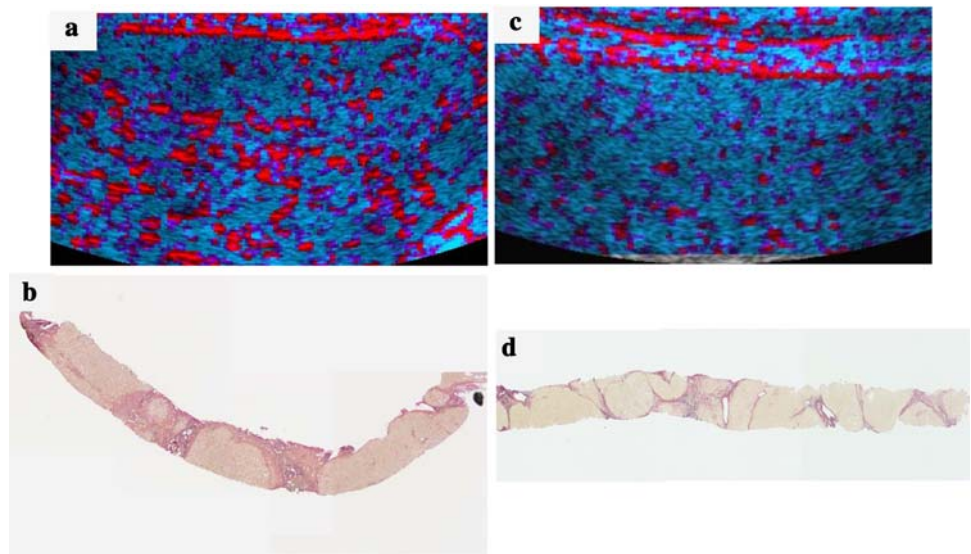
between any two of the three categories of septum thickness (Fig. 7b).

Biopsy specimens from two cirrhotic patients with different US-Red% were examined in detail (Fig. 8). In Case 1, US-Red was markedly seen on the color image (Fig. 8a), with US-Red% being as high as 9.8%. The liver biopsy specimen (Fig. 8b) of this case was rated as “large” in terms of nodule size and “thick” in terms of fibrous septum thickness. In Case 2, on the other hand, US-Red was less marked on the color image (Fig. 8c), with US-Red% being low (4.0%). The liver biopsy specimen (Fig. 8d) of this case was rated as “small” in terms of nodule size and “thin” in terms of fibrous septum thickness. Thus, pathological differences were noted between Cases 1 and 2.

Discussion

The echo patterns of liver parenchyma are composed of minute and complex scattering. Furthermore, because there are various changes in liver tissue, it is not easy to specify a

Fig. 8 Example of two cirrhotic cases. Case 1. **a** Color image showing much *red scatter* (US-Red). **b** Liver biopsy showing large nodules and a wide fiber septum (EVG $\times 40$). Case 2. **c** Color image showing little *red scatter* (US-Red). **d** Liver biopsy showing small nodules and a narrow fiber septum (EVG $\times 40$)



certain type of tissue change readily from a change in echo pattern. Because of this, ultrasound has been used in various studies to evaluate tissue characterization of the liver. Although characteristic ultrasound images of liver cirrhosis, etc., which currently serve as indicators for ultrasound diagnosis, have been reported in qualitative studies on echo patterns and histopathological findings [1–5], the ultrasound diagnosis is highly dependent on the examiner's knowledge and skill. On the other hand, a correlation between histological changes and acoustic characteristics has been reported in quantitative studies using statistical analysis of RF signal amplitude (a more objective method of evaluation) [11–17], but this correlation has not yet been made use of in clinical practice. One reason is the difficulty of linking the results of statistical analysis to findings from B-mode images. New approaches and reviews from a clinical standpoint are needed to achieve this. Therefore, this study was undertaken by applying statistical analysis of RF signal amplitude using the ASQ method. Lesions out of the innumerable speckle signals were selected and highlighted on B-mode images using specific colors to enable detailed analysis. These images were then compared with histopathological findings from biopsy specimens.

The ASQ method is designed to enable analysis of RF signals in each of the many small ROIs set within a large ROI for the purpose of improving the accuracy of analysis. We used this method and selected small ROIs with a high degree of deviation from the Rayleigh distribution. These small ROIs were seemingly reflecting advanced lesions, and represented on B-mode images by red scatter (US-Red). The signals contained in these small ROIs are non-homogeneous in intensity, and some are of abnormal intensity. These high-intensity signals are produced on the acoustic reflectional plane formed at the interface of two

materials with a large difference in acoustic impedance. It was therefore not irrational to consider that US-Red reflects an acoustic reflectional plane that is caused by some local tissue structure. We predicted that this tissue structure was primarily made of fibrous tissue, and so we first analyzed the relationship between US-Red and fibrous tissue.

When the percentage of the image area occupied by US-Red (US-Red%) was calculated and analyzed, it was shown that the increase in US-Red% was closely correlated with the progression of liver fibrosis stage. This finding suggests that US-Red increases as a result of fibrous expansion of Glisson's sheath and the formation of a fibrous bridge and septum that determine the liver fibrosis stage. These tissue structures were estimated to be primarily responsible for formation of the acoustic reflectional plane that generates echo signals of abnormally high intensity. Although we also expected a correlation between US-Red% and percent liver fibrosis, no significant correlation existed between them. These results suggest that the increase in US-Red% is attributable to an increase in the acoustic reflectional plane because of formation of a fibrous bridge and septum, rather than a simple increase in fibers. Regarding the acoustic reflectional plane, Hachiya and Yamaguchi et al. [20, 21] reported that the speed of sound through fibrous tissue is higher than that through regenerated nodules of the cirrhotic liver, suggesting that the interface between them serves as the acoustic reflectional plane, resulting in reflection of abnormally high intensity. This result from a basic study supports the view that a fibrous bridge and septum can be responsible for formation of the acoustic reflectional plane.

These findings suggest that US-Red% can provide an objective and non-invasive means of assessing the progression of liver fibrosis stage in patients with chronic liver

disease. Still more, if B-mode images are checked for US-Red (expressed in color), it will be possible to visually collect information reflecting the fibrous structures forming the acoustic reflectional plane, thus making it easier to speculate about the disease stage. In this study the diameter of small ROIs was set at 1 mm (almost equal to the diameter of liver lobules). If the method for image analysis is modified and more detailed pathological evaluation is made, this technique is expected to allow qualitative and objective evaluation of fibrosis-associated changes in tissue structure. This technique will yield information useful for many clinicians involved in the management of chronic liver disease.

As illustrated above, the results from this study suggest that US-Red% is useful for estimating the progression of liver fibrosis stage. However, we cannot ignore the fact that US-Red% varies widely among different cases of liver cirrhosis. In view of this variation, it is difficult to say that US-Red% can replace liver biopsy as a means of diagnosing liver cirrhosis. For non-invasive diagnosis of liver cirrhosis, it seems more useful in clinical practice to make a general assessment based on conventionally reported ultrasonographic features of cirrhosis (liver atrophy, bluntness of liver edge, morphological changes on the liver surface such as elevation and depression, and so on) with hematological data (platelet count, etc.).

However, from the viewpoint of detecting histological changes on ultrasound images, it is quite noteworthy that US-Red% varies widely among cases of liver cirrhosis, although these cases were uniformly rated at F4 histopathologically. As stated above, US-Red% reflects an increase in the acoustic reflectional plane because of fibrosis rather than the absolute amount of fibers. If this point is taken into account, we may say that patients with liver cirrhosis have a variety of acoustic reflectional planes. Therefore, regarding the cause of the variation in US-Red% among different cases of liver cirrhosis, we may say that US-Red is more abundant in cases of macronodular cirrhosis because the acoustic reflectional plane formed at the interface between the fibrous septum and nodules is broader. We may also say that US-Red is not correspondingly abundant in cases where the arrangement of fibers is markedly disturbed under the influence of necrotic inflammation or in cases of micronodular cirrhosis where extensive fiber is not dense but minute, because reflection, scattering, retraction, and interference increase in these cases, reducing the degree of deviation from the Rayleigh distribution in the echo signal analysis. We postulate that US-Red% is low for some cases of liver cirrhosis (close to that of F1 cases) because of an acoustic mechanism. If the validity of this view is endorsed, it will be possible to make a detailed assessment of current tissue structure with this technique and a more clinical evaluation of disease activity in cases diagnosed as having

liver cirrhosis on the basis of liver morphology, hematology, etc., and cases previously diagnosed as having liver cirrhosis based on histological findings.

In patients with liver disease, lesions composed of various minute structures are not simple or uniform but are diverse and can change from time to time. If US-Red% is further analyzed pathologically and the value set for US-Red% is optimum, it will be useful as a clinical indicator enabling not only staging of fibrosis but also non-invasive assessment of various lesions of liver tissue.

Conclusion

For the purpose of evaluating tissue characterization of the liver using ultrasound, we devised a method by which the information reflecting the acoustic reflectional plane is represented in color on B-mode images. The findings obtained by this technique were compared with pathological findings. The results of analysis of such color images suggest that this technique is useful for estimating the progression of liver fibrosis stage (F1–3) and evaluating nodule size in patients with liver cirrhosis. In addition, this technique requires only simple analyses and manipulations and enables visual assessment of lesions indicated by the acoustic reflectional plane. This technique with these features will be clinically beneficial and merits further evaluation.

Acknowledgments The authors are indebted to ultrasound technologists at the Clinical Physiology Laboratory and members of the Pathology Division of Toho University Omori Medical Center for their cooperation with this study.

References

1. Freeman MP, Vick CW, Taylor KJ, Carithers RL, Brewer WH. Regenerating nodules in cirrhosis: sonographic appearance with anatomic correlation. *Am J Roentgenol.* 1986;146:533–6.
2. Nakajima M, Murata H, Nagai M, et al. Relationship between parenchymal echo patterns and histological findings of the liver in patients with liver cirrhosis. *Jpn J Med Ultrason.* 1989;16:161–9. (in Japanese).
3. Takao K, Masaaki E, Masao O, et al. Classification of liver cirrhosis based on parenchymal echo patterns and its clinical usefulness for diagnosis of liver cirrhosis. *Jpn J Gastroenterol.* 1989;86:1473–85. (in Japanese).
4. Ishikawa H, Ono M, Goto M, et al. Ultrasonographic findings in patients with liver cirrhosis; relationships between parenchymal, superficial echo patterns, and histological findings. *Jpn J Med Ultrason.* 1990;17:522–9. (in Japanese).
5. Moriya M. Correlation between parenchymal echographic pattern and pathological findings in chronic liver disease B and C. *J Tokyo Women's Med Univ.* 1993;63:286–91. (in Japanese).
6. Kusano M. Ultrasonographic diagnosis of liver disease; color Doppler imaging of peripheral liver blood flow. *J Med Soc Toho Univ.* 2001;48:140–6.

7. Shinohara M. Determination of peripheral color signal density using contrast-enhanced color Doppler ultrasonography in diffuse liver disease. *J Med Ultrason*. 2004;31:53–8. (in Japanese).
8. Tanigawa K, Ishii K, Sumino Y. Determination of peripheral vessel divergence angle with Levovist in diffuse liver disease. *J Med Ultrason*. 2007;34:165–70. (in Japanese).
9. Fujita Y, Yoshizawa K, Nakajima S, et al. Evaluation of Kupffer cells function of liver with Sonazoid[®]-enhanced ultrasonography. *Rad Fan*. 2007;5:50–2. (in Japanese).
10. Yoshizawa K, Fujita Y, Nakajima S, et al. Evaluation of hepatic parenchymal perfusion with Sonazoid[®]-enhanced ultrasonography in diffuse liver disease. *Rad Fan*. 2007;5:47–9. (in Japanese).
11. Yamaguchi T, Hachiya H, Kamiyama N, et al. Examination of the spatial correlation of statistics information in the ultrasonic echo from diseased liver. *Jpn J Appl Phys*. 2002;41:3585–9.
12. Yamaguchi T, Hachiya H, Kamiyama N, et al. Estimation of characteristic of echo envelope using RF echo signal from the liver. *Jpn J Appl Phys*. 2001;40:3900–4.
13. Yamaguchi T, Fukamachi K, Imaizumi S, et al. The comparison between the estimation result of echo information and clinical diagnosis of diffused liver diseases. vol. 102. Technical Report of IEICE No. 411:US2002-64. 2002. p. 7–12.
14. Kamiyama N, Yamaguchi T, Hachiya H. Tissue characterization using statistical information from ultrasound echo signals. *Med Imaging Technol*. 2003;21:112–6. (in Japanese).
15. Fujii Y, Taniguchi N, Takano R, et al. Texture analysis with the new method of segments the region of interest into multiple layers for RF amplitude histogram analysis in the fibrous liver of rats. *J Med Ultrason*. 2001;28:J681–91. (in Japanese).
16. Fujii Y, Taniguchi N, Itoh K, et al. Quantitative processed images acquired by histogram-SNR imaging used to evaluate parenchymal heterogeneity in the liver. *J Med Ultrason*. 2003;30:13–9.
17. Toyoda H, Kumada T, Kamiyama N, et al. Evaluation of liver fibrosis in patients with chronic hepatitis C on B-mode images using an algorithm based on statistical analysis of ultrasound signals. *Am J Roentgenol*. 2009;193:1037–43.
18. Ichida F, Tsuji T, Omata M, New Inuyama Classification, et al. New criteria for histological assessment of chronic hepatitis. *Int Hepatol Commun*. 1996;6:112–9.
19. Burckhardt CB. Speckle in ultrasound B-mode scans. *IEEE Trans Sonics Ultrason*. 1978;SU-25:1–6.
20. Hachiya H, Yamaguchi T. Acoustic characteristics of the tissue and the ultrasonic B-mode image. *Med Imaging Technol*. 2003;21:95–100. (in Japanese).
21. Yamaguchi T, Hachiya H. A case of measurement of acoustic properties in cirrhotic liver specimen. *Jpn J Med Ultrason*. 2008;35:33–4. (in Japanese).